

Dust levitation in an inverse sheath

Rinku Deka and Madhurjya P Bora

*Physics Department, Gauhati University, Guwahati 781014, India**

The results of an analysis of the physics of levitation of negatively charged dust particles over a surface (wall) in an inverse sheath are reported. It is shown that under suitable parameter regime, the ion-drag force may balance the combined electrostatic and gravitational force on the dust particles owing to its hollow profile as one moves away from the surface. Our analysis shows that the parameter regimes in which such a situation may result is realizable in laboratory and space plasma environments, particularly the near-surface dayside lunar plasma. The lunar surface and dust grains are electrostatically charged due to the interaction with the solar wind plasma environment and the photoemission of electrons due to solar UV radiation. This results in a process that charges the surface positively and generates a near-surface photoelectron inverse plasma sheath. The potential structure changes from a monotonic classical sheath to an inverse sheath as the emitted electron density becomes larger than the plasma electron density. In a relatively newer, recently developed charging model, called the Patched Charge Model, it has shown both theoretically and experimentally that even in photoelectron-rich environment, dust particles lying on a regolith surface can attain large negative potential due to formation of micro cavities. This negative potential may reach such values so that dust mobilization and lofting may become possible. In our work, we have assumed the existence of such negatively charged dust particles in a photoelectron-rich environment and argue that once the dust lofting is effected, the levitation can be sustained through the ion-drag force. The conditions of levitation are investigated for these dust particles and the levitation distances from the lunar surface are calculated.

I. INTRODUCTION

The subject of plasma-wall interaction has always been an intriguing one. The plasma sheath, which usually forms in the vicinity of a surface, is a site of intense nonlinear activities. In general, the wall becomes negatively charged and a classical plasma sheath is formed¹. However, when there are emissions from wall such as secondary electron emission and photoemission, the wall becomes positively charged and an inverse sheath is formed². In this work, we discuss the dynamics of negatively charged dust particles in such an inverse sheath. As an example case, we take the case of lunar plasma sheath, though the work can be relevant in other laboratory and space plasmas, as well.

Devoid of any detectable atmosphere, the lunar surface is constantly in interaction with the solar wind plasma and solar ultraviolet (UV) radiation and it serves as an ideal natural environment for studying plasma-wall interaction. On the sunlit side, the lunar surface collects solar wind ions and electrons as well as is also subjected to photoemission. Primarily due to the solar UV photons, photoelectrons are emitted from the lunar surface and the surface potential becomes positive. These photoelectrons create a sheath above the dayside lunar surface with a barrier of negative potential³. If the ratio of the emitted electrons to the collected electrons is small, then the surface potential is negative relative to the plasma. In this case, a monotonic classical sheath is formed. When the emitted electron density becomes larger than the collected electron density, the potential structure becomes a monotonic inverse sheath, where the surface potential is more positive than the ambient plasma potential². Some of the early works towards understanding of the sheath dynamics include the works of Hobbs and Wesson⁴, who made a fundamental fluid theory for sheath in the presence of emitted electrons in case of a planar surface which was immersed in a plasma that consists of cold ions and Maxwellian electrons. Works of many authors⁵ contributed toward significant analytical insights to the photoelectron sheath over the lunar surface. Further computational studies^{6,7} include results from Particle-In-Cell (PIC) simulations of photoelectron sheath on lunar surface under different conditions.

So far as the investigation about dust-plasma interactions in laboratory plasmas are concerned, there are quite a number of important works, which have contributed to our understanding about this⁸. On the experimental front, both space borne and laboratory experiments provided us with valuable information about the potentials in the electron-emitting sheaths^{9–11}. Some recent works which are devoted to dusty plasma physics in the near-surface lunar layer, which demonstrate that in the terminator region, a sheath-like plasma layer exists, resulting electric field which can cause lofting of dust particles of size $\sim 2 - 3 \mu\text{m}$ to about 30 cm^2 . A very recent work investigates the *absence of dead zone* (where dust particles can not rise) near the lunar latitude $\sim 80^\circ$.

Coming back to the issue of dust dynamics in a plasma sheath, we note that dust particles are ubiquitous to space and laboratory plasmas and the lunar plasma sheath is also no exception. Bombardment of the lunar surface by high energetic electrons and ions causes ejection of dust particles from the lunar regolith to the plasma sheath. The movement of active dust transport near surfaces of airless bodies in the solar system including dust grains levitated above the lunar surface was first observed by the Surveyor spacecraft and the Apollo missions^{12–15}. The dust particles are abundant in all kinds of plasmas and it changes the plasma dynamics by being a constituent plasma component. From various satellite observations like Lunar Prospector (LP)¹⁶ and Apollo-Era Missions^{17–19}, we came to know about the existence of a complex as well as coupled plasma and layers of dust particles above the lunar surface^{13,20}. These micron and sub-micron sized dust grains from the lunar regolith get charged due to collection of electrons and ions from the plasma, photoemission, and secondary electron emission. In some recent works^{21,22}, the charge balance over the lunar surface and levitation of dust particles along with the steady state altitude dependence of dust density and particle size in the case of classical sheath have been investigated.

In this work, we present an analysis of the dynamics of *negatively charged* dust particles in an inverse sheath. As mentioned above, an inverse sheath usually forms on the dayside of the lunar surface due to photoemission. It is customary to assume that the dust particles in an inverse sheath also charge to positive potential due to the dust photoemission. While this is mostly true, there are situations where dust particles in an inverse sheath can also charge to high negative potential. One of the newest model on dust charging which has been developed is the *Patched Charge Model* (PCM), which can account for existence for dust particles with large negative charge in an environment which supports emission and absorption of photoelectrons. An example such a situation is the lunar plasma environment and lunar horizon glow³ is such a phenomena which may have an explanation through the PCM^{23?, 24}. In our work, we consider such a situation, where we have self-consistently calculated the dust-charge from the current-balance equations. Our analysis shows that the ion-drag force on the dust particles can sustain a levitation of even negatively charged particles in an inverse sheath and the combined effect of electrostatic, gravity, and ion-drag force can cause the dust particles of various sizes to levitate²⁵ and form *bands* above the lunar surface, the heights of which compare very well with the observational data^{15,26}. We believe that this is the first time that the possibility of levitation of negatively charged dust particles in an inverse sheath is reported.

In Sec II, we have considered our model and derived the electron and photoelectron density assuming both of them as Maxwellian. In Sec III, we have developed the potential structure and sheath equation. In Sec IV, we have considered the dynamics of the dust particles in the inverse sheath regime, where charging processes and current balanced are

self-consistently included. In this section, we have also calculated the various forces acting on a negatively charged dust grain when it is in the inverse sheath. We have also calculated the dust sizes with respect to the distances from the surface. In Sec V, we summarize our results.

II. PLASMA MODEL

We consider a one dimensional collisionless inverse plasma sheath consisting of electrons and ions with considerable presence of dust particles. As our region of interest is ion-acoustic time scale, the dust particles do not take part in the plasma dynamics. In 1-D, the basic equations are ion continuity, ion momentum, and Poisson's equation,

$$\frac{\partial n_i}{\partial t} + \frac{\partial}{\partial x}(n_i u_i) = 0, \quad (1)$$

$$\frac{\partial u_i}{\partial t} + u_i \frac{\partial u_i}{\partial x} = -\frac{1}{m_i n_i} \frac{\partial p_i}{\partial x} - \frac{e}{m_i} \frac{\partial \phi}{\partial x}. \quad (2)$$

The two populations of electrons — the plasma electrons (density n_{pe}) and the photoelectrons (density n_{ph}) emitted by the wall, are assumed to be Maxwellian, described by their respective distributions⁵,

$$f_{pe}(x, \mathbf{v}) = n_{pe0} \left(\frac{m_e}{2\pi T_e} \right)^{3/2} e^{-(m_e v^2 / 2 - e\phi) / T_e} \quad (3)$$

$$f_{ph}(x, \mathbf{v}) = n_w \left(\frac{m_e}{2\pi T_{ph}} \right)^{3/2} e^{-m_e v^2 / (2T_{ph}) + e(\phi - \phi_w) / T_{ph}}, \quad (4)$$

where $T_{e,ph}$ are electron and photoelectron temperatures (expressed in energy units), ϕ is the plasma potential, and ϕ_w is the potential at the wall. For an inverse sheath, the potential $\phi_w > 0$ and monotonically reduces to zero at the bulk plasma. We assume that far away from the wall, the plasma quasi-neutrality is maintained by the plasma electrons, photoelectrons, ions, and the charged dust particles,

$$n_{e0} + z_d n_d = n_{i0}, \quad n_{pe0} + n_{ph0} = n_{e0}, \quad (5)$$

where the subscript '0' denotes bulk plasma values. While the dust density is *not* a dynamic quantity but the dust charge number z_d is and z_{d0} denotes its value in the bulk plasma away from the wall. Both plasma electron and photoelectron densities can be assumed to be close to Boltzmannian. While the plasma electron is described by a single population, photoelectron density is described by two populations — a sheath-limited population and one which contribute to the bulk plasma electrons,

$$\begin{aligned} n_{pe} &= \int_{-\infty}^{\infty} \int_{-\infty}^{\infty} \int_{\sqrt{2e\phi/m_e}}^{\infty} f_{pe}(x, \mathbf{v}) d\mathbf{v} \\ &= \frac{1}{2} n_{pe0} e^{e\phi/T_e} \operatorname{erfc} \left(\frac{e\phi}{T_e} \right)^{1/2}, \end{aligned} \quad (6)$$

$$\begin{aligned} n_{ph} &= \int_{-\infty}^{\infty} \int_{-\infty}^{\infty} \int_{\sqrt{2e\phi/m_e}}^{\infty} f_{ph}(x, \mathbf{v}) d\mathbf{v} + 2 \int_{-\infty}^{\infty} \int_{-\infty}^{\infty} \int_0^{\sqrt{2e\phi/m_e}} f_{ph}(x, \mathbf{v}) d\mathbf{v} \\ &= \frac{1}{2} n_w e^{e(\phi - \phi_w) / T_{ph}} \left[1 + \operatorname{erf} \left(\frac{e\phi}{T_{ph}} \right)^{1/2} \right] = \frac{1}{2} n_{phw} e^{e\phi/T_{ph}} \left[1 + \operatorname{erf} \left(\frac{e\phi}{T_{ph}} \right)^{1/2} \right], \end{aligned} \quad (7)$$

where n_w is the photoelectron density at the wall and is related to the bulk photoelectron density through the relation $n_{phw} = n_w e^{-e\phi_w/T_{ph}}$. Note that the photoelectron density moving away from the wall (when they are produced) is half of the total photoelectrons produced which contribute to the bulk plasma. Similarly, the plasma electron density moving toward the wall (far away from the wall, at ∞) is half of the bulk electrons at ∞ . The ions are assumed to be polytropic,

$$p_i \propto n_i^\gamma. \quad (8)$$

However, as the temperature remains constant, in what follows, we assume $\gamma = 1$. The model is closed by the Poisson equation,

$$\epsilon_0 \frac{\partial^2 \phi}{\partial x^2} = e(n_{pe} + n_{ph} - n_i + z_d n_d). \quad (9)$$

Note that the dust density n_d is not a dynamical variable. We choose to normalize the ion density by the equilibrium values $n_{i0} \equiv n_0$, the plasma potential by T_e/e , length by Debye length λ_D , velocity by ion-thermal velocity $u_s = \sqrt{T_e/m_i}$, and time by λ_D/u_s . So, Eqs.(1,2) and (6,7) can be normalized as,

$$\frac{\partial n_i}{\partial t} + \frac{\partial}{\partial x}(n_i u_i) = 0, \quad (10)$$

$$\frac{\partial u_i}{\partial t} + u_i \frac{\partial u_i}{\partial x} + \frac{\sigma}{n_i} \frac{\partial p_i}{\partial x} = -\frac{\partial \phi}{\partial x}, \quad (11)$$

$$n_{pe} = \frac{1}{2} \delta_{pe} e^\phi \operatorname{erfc}(\phi^{1/2}), \quad (12)$$

$$n_{ph} = \frac{1}{2} \delta_{ph} e^{\phi/\sigma_{ph}} \left[1 + \operatorname{erf} \left(\frac{\phi}{\sigma_{ph}} \right)^{1/2} \right], \quad (13)$$

where $n_{pe,ph}$ are densities of the plasma electrons and photoelectrons normalized by the equilibrium electron density n_{e0} , $\delta_{pe,ph} = n_{pe0,ph0}/n_{e0}$ is a measure of the fraction of plasma and photoelectron densities to that of total bulk plasma electron density. The electron density at any instant is $n_e = n_{pe} + n_{ph}$. Note that $(\delta_{pe} + \delta_{ph})/2 = 1$. The normalized Poisson equation is given by,

$$\frac{\partial^2 \phi}{\partial x^2} = n_{pe} + n_{ph} - \delta_i n_i + \delta_d z_d,$$

where $\delta_{i,d} = (n_0, z_{d0} n_d)/n_{e0}$ are fractions of ion and dust densities to the bulk plasma electron density. The dust charge number is expressed in terms of its value in the bulk plasma. The ion pressure is normalized to $n_0 T_i$ and $\sigma = T_i/T_e$.

III. THE POTENTIAL STRUCTURE AND SHEATH EQUATION

Far away from the boundary, the plasma potential vanishes i.e. as $x \rightarrow \infty$, $\phi \rightarrow 0$, $u \rightarrow M$, $p_i \rightarrow 1$, $n_i \rightarrow 1$, $z_d \rightarrow 1$, where M is the mach number. In a co-moving frame of the wave, we have from Eqs.(10,11),

$$\frac{\partial}{\partial x}(n_i u_i) = 0, \quad (14)$$

$$-u_i \frac{\partial u_i}{\partial x} + \frac{\sigma}{n_i} \frac{\partial p_i}{\partial x} = -\frac{\partial \phi}{\partial x}, \quad (15)$$

From the continuity equation and integrating the Eq.(15) we have,

$$n_i = \frac{M}{\sqrt{\sigma W(z)}}, \quad z = \frac{M^2}{\sigma} \exp \left(\frac{M^2 + 2\phi}{\sigma} \right), \quad (16)$$

where $W(z)$ is the Lambert-W function and we have used the relation $u_i = M/n_i$. The dependence of n_i with the distance from the wall is shown in Fig.1. Integrating the Poisson's equation, we have

$$\frac{1}{2} \left(\frac{d\phi}{d\xi} \right)^2 + V(\phi, M, \sigma, \delta_i, \sigma_{ph}, \delta_{ph}) = 0, \quad (17)$$

where V is the Sagdeev or pseudo potential²⁷,

$$\begin{aligned} V(\phi, M, \sigma, \delta_i, \sigma_{ph}, \delta_{ph}) &= \left(1 - 2\sqrt{\phi/\pi} - e^\phi \operatorname{erfc} \sqrt{\phi} \right) \left(1 - \frac{1}{2} \delta_{ph} \right) + \frac{1}{2} \delta_{ph} \sigma_{ph} \xi(\phi) \\ &+ \delta_i \int_0^\phi n_i(\phi) d\phi + (1 - \delta_i) \int_0^\phi z_d(\phi) d\phi, \end{aligned} \quad (18)$$

and

$$\xi(\phi) = 1 - e^{\phi/\sigma_{ph}} \left(1 + \operatorname{erf} \sqrt{\phi/\sigma_{ph}} \right) + 2 \left(\frac{\phi}{\pi \sigma_{ph}} \right)^{1/2}, \quad (19)$$

The pseudo potential V satisfies the boundary condition $V|_{\phi=0} = 0$. Besides, V must be negative for all ϕ for a physically viable potential profile.

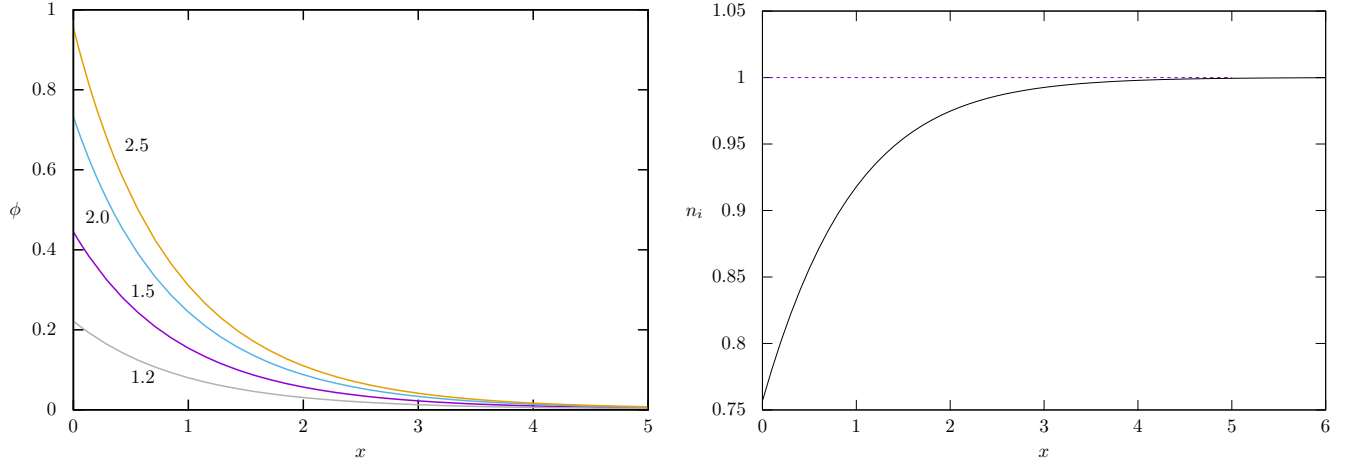


Figure 1. The potential profile (left) showing the formation of inverse sheath (the wall is at $x = 0$). The parameters used are $n_{e0} = 10^{12} \text{ m}^{-3}$, $T_e = 1 \text{ keV}$, $J_{h\nu} = 4.5 \mu\text{A}/\text{m}^2$, $M = 1.2$, $\sigma = 1$, $\delta_i = 1.1$, $\sigma_{\text{ph}} = 1$. The numbers in the figure indicates δ_{ph} . The panel on the right shows the normalized ion density as one moves from the wall. All the parameters are same with $\delta_{\text{ph}} = 2.5$.

A. Wall potential

To determine the wall potential, we employ the boundary condition at infinity (at a distance far away from the wall) where the fluxes for primary electrons, ions, and secondary electrons balance to have the net plasma current density zero. In our case the secondary electrons are the photoelectrons emitted by the wall,

$$J_{\text{pe}} + J_i + J_{\text{ph}} = 0, \quad (20)$$

where

$$J_{\text{pe}} = e \int_{-\infty}^{\infty} \int_{-\infty}^{\infty} \int_{-\infty}^0 f_{\text{pe}}(\infty, \mathbf{v}) d\mathbf{v} = -en_{\text{pe}0} \left(\frac{T_e}{2\pi m_e} \right)^{1/2}, \quad (21)$$

$$J_{\text{ph}} = e \int_{-\infty}^{\infty} \int_{-\infty}^{\infty} \int_{\sqrt{2e\phi_w/m_e}}^{\infty} f_{\text{ph}}(0, \mathbf{v}) d\mathbf{v} = en_w \left(\frac{T_{\text{ph}}}{2\pi m_e} \right)^{1/2} e^{-e\phi_w/T_{\text{ph}}}, \quad (22)$$

$$J_i = en_0 M \left(\frac{T_e}{m_i} \right)^{1/2}. \quad (23)$$

Note that the sheath-limited photoelectrons do not contribute to the net plasma current. Eq.(20) can be written in a normalized form as

$$\phi_w = \sigma_{\text{ph}} \ln \left[\delta_m \delta_w \left(\frac{1 + \sqrt{\sigma_{\text{ph}}}}{2\delta_m - \delta_i M \sqrt{2\pi}} \right) \right] = \sigma_{\text{ph}} \ln \left(\frac{\delta_w}{\delta_{\text{ph}}} \right) \quad (24)$$

which determines the wall potential ϕ_w . $\delta_m = \sqrt{m_i/m_e} \approx 43$. In Fig.1, we show the structure of the plasma potential ϕ which shows the formation of inverse sheath. In the figure, the wall is at $x = 0$.

IV. DUSTS IN PLASMA SHEATH

A. Current balance

We now consider various currents to the surface of the dust grains which are due to electrons (I_e), ions (I_i), photoelectrons from the wall (I_{ph}), and the photoemission current emitted by the dust grain itself ($I_{h\nu}$). We assume that the currents to the surface of the dust particles remain balanced all throughout,

$$\sum I = 0 = I_e + I_i + I_{\text{ph}} + I_{h\nu}. \quad (25)$$

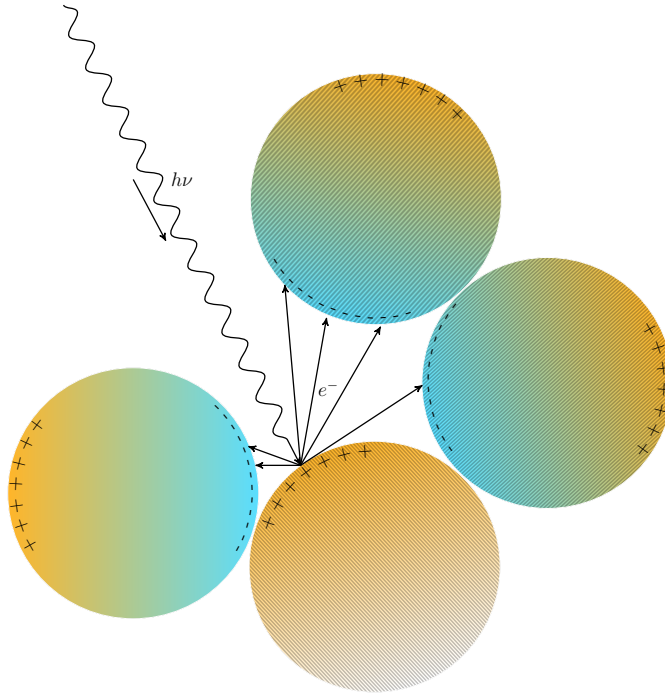


Figure 2. A schematic representation of the Patched Charge Model.

This can be justified in the parameter space where this analysis is relevant. For negatively charged dust particles, the expressions for the currents are given by²⁸,

$$I_e = -4\pi r_d^2 e n_{pe} \left(\frac{T_e}{2\pi m_e} \right)^{1/2} e^{e\phi_d/T_e}, \quad (26)$$

where ϕ_d is the dust potential and r_d is the average radius of a dust particle,

$$I_i = 4\pi r_d^2 e n_i \left(\frac{T_i}{2\pi m_i} \right)^{1/2} \left(1 - \frac{e\phi_d}{T_i} \right), \quad (27)$$

$$I_{h\nu} = \pi r_d^2 J_{h\nu}, \quad (28)$$

where $J_{h\nu} = e J_p Q_{ab} Y_p$ is the photoemission current density. Here J_p is the photon flux, Q_{ab} is the efficiency of absorption for photons which is ~ 1 , and Y_p is the photoelectron yield. For lunar dust $J_{h\nu} \sim 4.5 \mu\text{A}/\text{m}^2$ ²⁹,

$$I_{ph} = -4\pi r_d^2 e n_{ph} \left(\frac{T_{ph}}{2\pi m_e} \right)^{1/2} e^{e\phi_d/T_{ph}}. \quad (29)$$

Using the expression for $n_{pe,ph}$ from Eqs.(12,13), the normalized current balance equation can be written as,

$$-\delta_{pe} \delta_m e^{\phi+\phi_d} \text{erfc}(\phi^{1/2}) + 2n_i \delta_i \sqrt{\sigma} \left(1 - \frac{\phi_d}{\sigma} \right) + \sqrt{\pi/2} \tilde{J}_{h\nu} - \delta_{ph} \delta_m e^{(\phi+\phi_d)/\sigma_{ph}} \left[1 + \text{erf} \left(\frac{\phi}{\sigma_{ph}} \right)^{1/2} \right] = 0, \quad (30)$$

where $\tilde{J}_{h\nu}$ is the normalized photoemission current density. Note that the dust charge $Q_d = q_d z_d$ is related to the relative dust potential ϕ_d as (assuming a spherical dust grain) $Q_d \equiv C \phi_d = 4\pi \epsilon_0 r_d \phi_d$, $\phi_d = \phi_g - \phi$, where C is the capacitance of the spherical dust grain and ϕ_g is the absolute grain potential (with respect to zero). The dust charge number z_d , thus can be expressed in terms of the dust potential ϕ_d relative to the dust charge number at zero potential $z_d(\phi) = \phi_d(\phi)/\phi_{d0}$, where $\phi_{d0} = \phi_d(\phi)|_{\phi=0}$.

B. Inverse sheath and the Patched Charge Model

As has been already mentioned, we note that there are phenomena related to dust in astrophysical environments, which are not adequately explained by classical dust charging models. One of the newest model which has been

developed is the *Patched Charge Model* (PCM)^{23,24}, which can account for existence of dust particles with large negative charge in an environment which supports emission and absorption of photoelectrons.

In the usual case, it is customary to assume that the dust particles be positively charged due to emission of photoelectrons following the same procedure which charges the lunar regolith to a positive potential on the dayside, resulting the existence of an inverse sheath. However, the PCM can explain why, even in such an environment, the dust particles on such regolith surfaces may attain large negative potential. In the PCM, there are formation of *micro cavities* created by the voids between the dust particles which can create large negative electric field due to absorption of photoelectrons (which are emitted by a neighboring dust particle) by the *inner* surface of the surrounding dust particles (see Fig.2). The basic principle of the PCM has already been verified through various laboratory experiments²³, which can be used to investigate the phenomena of levitation of negatively charged dust particles in the presence of an inverse sheath. The emission of photoelectrons by the *inner* particles in the micro cavities and absorption of these photoelectrons by the dust particles lying on the surface, may charge the dust particles on the surface to enormously high net negative potentials despite their *outer* surface being charged to a positive potential by the incoming UV photons. The laboratory experiments, simulating the lunar regolith surface shows that this inter-particle negative electric field is enough to cause dust mobilization and lofting up to about 0.11 m above the surface²³. We further argue that once the initial mobilization is effected causing lofting of the dust particles above the surface, the ensuing ion-drag force will be able to sustain the levitation and push it further up until the net force becomes zero and a stable levitation height is obtained. While considering this scenario, we assume that the lofted dust particles will have the same amount of net negative charge, which they accumulated at the regolith surface. In what follows, we shall assume that the dust particles are negatively charged despite being present in a photoelectron-rich environment.

C. Forces on the dust particles

In this section, we calculate the forces on a dust particle assume it to be negatively charged. The primary forces which act on a dust particle immersed in a plasma are electrostatic (\mathbf{F}_E), gravity (\mathbf{F}_g), polarization (\mathbf{F}_{pol}), ion drag (\mathbf{F}_{ion}), and neutral drag (\mathbf{F}_n) force, so that the total force \mathbf{F} on a dust particle is given by²⁸,

$$\mathbf{F} = \mathbf{F}_E + \mathbf{F}_{\text{pol}} + \mathbf{F}_g + \mathbf{F}_{\text{ion}} + \mathbf{F}_n. \quad (31)$$

In what follows, we shall neglect $\mathbf{F}_{n,\text{pol}}$ as the neutral drag force is proportional to the dust thermal velocity u_d which is $\ll u_i$ and so in the ion-acoustic time scale, it can be safely neglected. Besides the polarization force is important *only* except in highly dense dusty plasmas and can be neglected. The normalization factor for force \mathbf{F} is conveniently expressed as $(4/3)\pi\lambda_D^3\rho_d g$, which is the total amount of gravitational force acting on dust particles, those are within a Debye sphere, ρ_d being the matter density of dust particles. The normalized expressions for $\mathbf{F}_{E,g}$ are given by,

$$\mathbf{F}_E = -3r_d R \phi_d \left(\frac{d\phi}{dx} \right), \quad (32)$$

$$\mathbf{F}_g = -r_d^3, \quad (33)$$

where R is a dimensionless parameter which represents the ratio of the thermal force on the electrons ($F_p = n_0 T_e / \lambda_D$) to the gravitational force ($F_g = \rho_d g$) on the dust particles,

$$R = \frac{F_p}{F_g} = \frac{n_0 T_e / \lambda_D}{\rho_d g}. \quad (34)$$

Note that the gravity acts downward *into* the sheath. The ion drag force is actually due to two factors — momentum transfer due to ion-dust collision (collection force \mathbf{F}_{coll}) and Coulomb scattering part of ion-dust collision (\mathbf{F}_{Coul}), which is given by (dimensional),

$$\mathbf{F}_{\text{ion}} = \mathbf{F}_{\text{coll}} + \mathbf{F}_{\text{Coul}}, \quad (35)$$

$$\mathbf{F}_{\text{coll}} = \pi b_{\text{max}}^2 m_i n_i \bar{u} \mathbf{u}_i, \quad \bar{u} = (u_i^2 + u_s^2)^{1/2}, \quad (36)$$

$$\mathbf{F}_{\text{Coul}} = 4\pi b_{\perp}^2 m_i n_i \bar{u} \mathbf{u}_i \ln \left(\frac{\lambda_D^2 + b_{\perp}^2}{b_{\text{max}}^2 + b_{\perp}^2} \right)^{1/2}, \quad (37)$$

where

$$b_{\text{max}} = r_d \left(1 - \frac{2e\phi_d}{m_i \bar{u}^2} \right)^{1/2}, \quad b_{\perp} = \frac{eQ_d}{4\pi\epsilon_0 m_i \bar{u}^2}. \quad (38)$$

Note that b_{\max} and b_{\perp} have dimensions of length. The normalized expression for \mathbf{F}_{ion} is given by,

$$\mathbf{F}_{\text{ion}} = \hat{\mathbf{l}} \frac{3}{4} R \bar{u} M \left[b_{\max}^2 + 2b_{\perp}^2 \ln \left(\frac{1 + b_{\perp}^2}{b_{\max}^2 + b_{\perp}^2} \right) \right], \quad (39)$$

where $\hat{\mathbf{l}}$ is the unit vector in the direction of \mathbf{u}_i .

As the inverse sheath is charged to a positive potential, the dust particles feel a downward (toward the sheath) pull due to gravity and the electric field, whereas the ion drag force acts away from the sheath. In Fig.3, we show the results of our numerical calculations for lunar plasma parameters — $T_e = 1 \text{ keV}^{30}$, $n_{e0} = 10^{12} \text{ m}^{-331}$, $J_{h\nu} = 4.5 \mu\text{A}/\text{m}^{229}$, and $\rho_d = 1000 \text{ kg}/\text{m}^{35}$ for two Mach numbers $M = 1.0$ and 1.5 . We note here that there are also reports about much higher photoelectron density of $\sim 2 \times 10^{14} \text{ m}^{-3}$ above the dayside lunar surface³². The panels on the left show the net force experienced by a dust particle which initially tends to be slight negative (downward, toward the sheath) for smaller dust particles. For larger dust particles, the net force is positive (upward, away from the sheath). For even larger dust particles, the net force again becomes negative pulling the massive dust particles down to the surface. This behavior can be understood on the basis of the fact that the accumulation of negative charges on a dust particles is proportional to its size, which increases the ion drag force and is responsible for levitation of the dust particles. However, as dust size grows, the force due to gravity becomes dominant as well as the electrostatic attractive force, which eventually win for the larger dust particles. The panels on the right show the contours of the net force \mathbf{F} experienced by the dust particles in the (r_d, x) parameter space, where the red arrows indicate the lines for $\mathbf{F} = 0$. What is interesting and a unique behaviour that we see is that formation of *dust-bands* (position where $\mathbf{F} = 0$) or *striations* at different heights as one moves upward from lunar surface, which is at $x = 0$. The bands or striations are caused by the profile of the ion-drag force which has a minima as one comes away from the surface (see Fig.4). In terms of physical distance, the bands (as seen in Fig.3) are formed at about $\sim 1.4, 1.9$, and 2.1 m from the lunar surface, with the Debye shielding length $\sim 0.23 \text{ m}$ for the assumed lunar plasma parameters, which compares very well with the reported levitation height of $\sim 2 \text{ m}$ for dust particles above the lunar surface³³ with an average size of $\sim 2 - 4 \mu\text{m}$ for the dust particles³⁰. The most important and significant finding of our calculations is that the levitating height of the dust particles remains same for a considerable size distributions of the dust particles, which is quite opposite of what is found in case of classical dust-levitation scenario with only electrostatic and gravitational force²¹. As can be seen from Fig.3 (upper panel), the levitation height remains reasonably constant for dust sizes from about $1.5 \mu\text{m}$ to $4.5 \mu\text{m}$ for a Mach number of 1.0 . This property of the dust-levitation causes formation of bands or striations and may have explanation to lunar phenomena such as the horizon glow.

We would like to note that the solar wind plasma has a thermal velocity of $\sim 300 \text{ km}/\text{s}$ with a bulk plasma velocity of about $\sim 400 \text{ km}/\text{s}^{34}$, which is toward the dayside lunar surface. This velocity is incorporated into the calculation through the Mach number, which is the velocity of the solar wind ions far away from the sheath. So, a Mach number of 1.2 results a bulk ion velocity of $\sim 380 \text{ km}/\text{s}$ and a velocity of $\sim 450 \text{ km}/\text{s}$ is equivalent to Mach number of ~ 1.4 . We have shown the formation of levitated dust bands even for a higher Mach number of $M = 1.5$.

1. An estimate of the ion-drag force

We now try to calculate the forces at the wall, $x = 0$, where x is the distance from the wall measured in the unit of λ_D . For dust matter density of $\sim 1000 \text{ kg}/\text{m}^3$, average dust radius of $\sim 10^{-6} \text{ m}$, $T_i \sim T_e \sim 1 \text{ keV}$, $n_0 \sim 10^{12} \text{ m}^3$, we find that

$$b_{\max} \simeq 7 \times 10^{-5} \quad \text{and} \quad \bar{u} \sim 1.7. \quad (40)$$

As such, the expression for F_{ion} becomes

$$F_{\text{ion}} \sim \frac{3}{4} R \bar{u} M b_{\max}^2. \quad (41)$$

For Mach no ~ 1 , we see that $F_{\text{ion}} \sim 4.8 \times 10^{-16}$ (normalized). A simple calculation shows that the force due to gravity $F_g \sim 7.7 \times 10^{-17}$, and that due to the electric field is $F_E \sim 6.8 \times 10^{-12}$. However, as one moves away from the surface, the force due to electric field on dust particles decreases as the dust potential becomes less negative (see Fig.4). Note that the dust potential is self-consistently calculated using the current balance condition (Eq.30 in the manuscript). In Fig.4, we have shown variation of the relative magnitudes of the forces with the distance from the wall. Clearly, as we move away from the surface, the the ion-drag force dominates and becomes capable of balancing the other two forces leading to dust levitation.

In this context, we would like to draw the attention to a very recent experimental work on ion-drag force on dust particles in laboratory plasmas, where the ion-drag force is found to be almost of the same order as the force due to

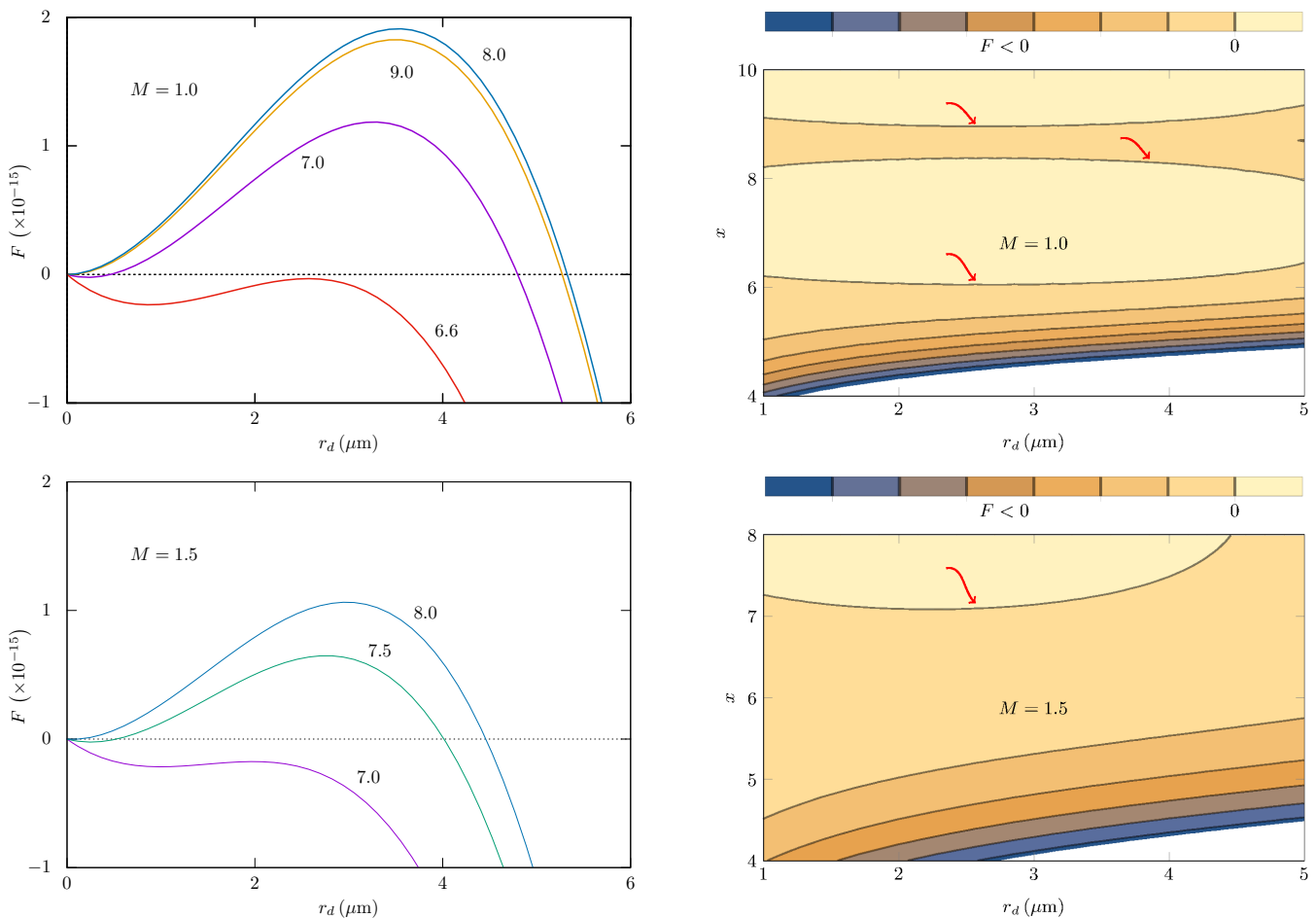


Figure 3. The levitation of dust particles above an inverse sheath for two Mach numbers 1.0 and 1.5. The left panels show the total force experienced by the dust particles. The inscribed numbers on the curves denote values of x . The parameters used here are for lunar surface. $n_{e0} = 10^{12} \text{ m}^{-3}$, $T_e = 1 \text{ keV}$, $J_{h\nu} = 4.5 \mu\text{A}/\text{m}$, $\sigma = 1$, $\delta_i = 1.1$, $\sigma_{\text{ph}} = 1$, $\delta_w = 1.5$. The right panels show the contours of total force \mathbf{F} for the shown parameter space. The red arrows indicate the lines where $\mathbf{F} = 0$.

the electric field and the force due to gravity (i.e. earth gravity) for similar plasma parameters⁸. We also note that the plasma parameters used in this work are also very well realizable in laboratory conditions.

V. SUMMARY AND CONCLUSION

In summary, a self consistent analytical model describing the inverse sheath structure over the lunar surface has been developed. We have presented the basic formulation for one dimensional collisionless inverse plasma sheath consisting of electrons and ions with considerable presence of dust particles. The electrons have two populations — the plasma electrons and the photoelectrons emitted by the wall. In our case, the plasma electron is described by a single population and photoelectron density is described by two populations — one which is sheath limited population and another which contribute to the bulk plasma electrons. The electron densities have been derived by assuming both the plasma electrons and photoelectrons populations to be Maxwellian. In deriving the sheath structure and dust levitation phenomena, a steady state potential over the lunar regolith has been determined. The dust charge has been consistently determined by balancing the currents to the surface of the dust particles. Our analysis has been found to be relevant in both laboratory and space plasma environments.

When the lunar surface is exposed to the solar UV radiation and solar wind plasma, the electrostatic charging of surface as well as the dust particles can lead to dust levitation under favourable circumstances. Previous charging models were unable to account for particle charges large enough to attain the kinds of motion observed either in space or in lab conditions^{35,36}. Laboratory based experiments have supported the “Patched Charge Model”, which can

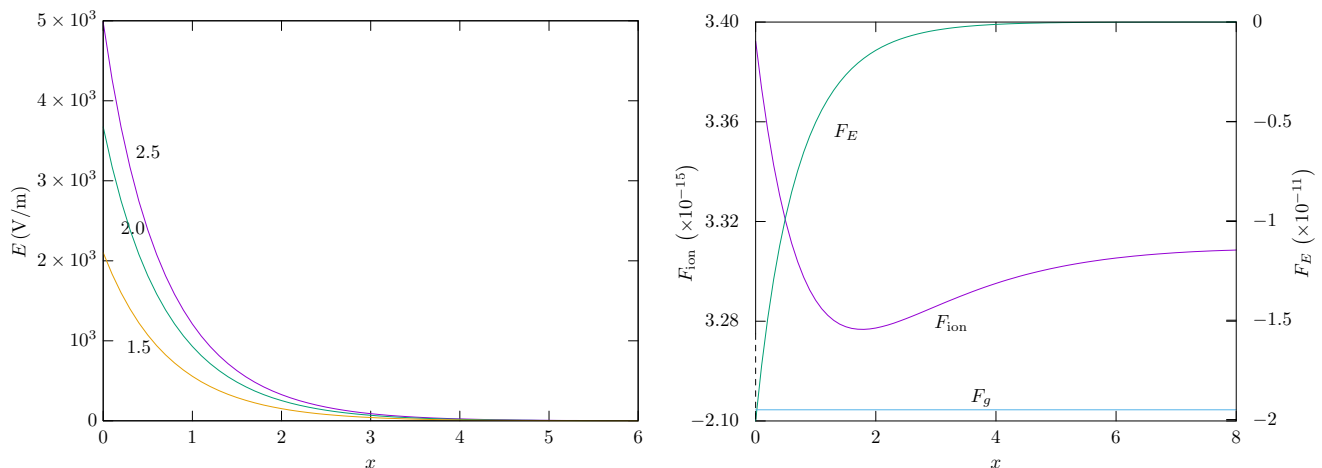


Figure 4. The electric field (left) is shown for the parameters $n_{e0} = 10^7 \text{ m}^{-3}$, $T_e = 1 \text{ keV}$, $J_{h\nu} = 4.5 \mu\text{A}/\text{m}^2$, $M = 1.2$, $\sigma = 1$, $\delta_i = 1.1$, $\sigma_{ph} = 1$. The numbers in the figure indicates δ_{ph} . The panel on the right shows the magnitudes of the three forces (normalized) for the same parameters and the dust particle size $3 \times 10^{-6} \text{ m}$.

explain why the dust particles lying on a regolith surface may attain large negative charge, even in a photoelectron-rich environment under favourable conditions. According to this model, micro cavities form between dust particles and the shielded surface patches amass large amounts of negative charge from photoelectrons and secondary electrons emitted by the surface layer patches with direct UV or electron beam exposure. The collected negative charge may become large enough to cause dust mobilization and dust lofting. We have argued that the ion drag force can sustain the levitation of negatively charged dust particles in an inverse sheath, once their initial lofting is effected due to large negative charge the dust particles may acquire following formation of micro cavities on the surface. Our analysis show that levitation of the negatively charged dust particles is possible in the inverse photoelectron sheath under favourable parameter space owing to the ion drag force on the dust particles. Though in most of the cases, the ion-drag force remains negligible, it can play an important role in suitable parameter regime as shown in this work and also in laboratory environments.

We have analytically determined the heights of the levitating dust grains from the surface of the moon with lunar plasma parameters. In our study, we have examined the levitation distance from the surface for different sizes of dust particles. In certain cases, there are more than one levitation heights leading to the formation of bands of dust particles above the surface. One important finding of our work is that the levitation heights of these negatively charged dust particles remain almost same for dust particles of different sizes, ranging from about $1.5 \mu\text{m}$ to $4.5 \mu\text{m}$, which support the formation of bands of dust particles over the lunar surface.

ACKNOWLEDGEMENT

It is a pleasure to thank the anonymous referee for a critical review of the manuscript. One of the authors, RD thanks UGC, India for the BSR Fellowship during which the work has been carried out.

* mpbora@gauhati.ac.in

¹ K. U. Riemann, *Journal of Physics D* **24**, 493 (1991).

² X. Wang, J. Pilewskie, H.-W. Hsu, and M. Horányi, *Geophysical Research Letters* **43**, 525 (2016).

³ R. H. Manka, in *Photon and Particle Interactions with Surfaces in Space*, edited by R. J. L. Grard, pages 347–361, Dordrecht, Reidel, 1973.

⁴ G. D. Hobbs and J. A. Wesson, *Journal of Plasma Physics* **9**, 85 (1967).

⁵ T. O. Nitter, O. Havnes, and F. Melandsø, *Journal of Geophysical Research* **103**, 6605 (1998).

⁶ A. Poppe and M. Horányi, *Journal of Geophysical Research* **115**, A08106 (2010).

⁷ A. R. Poppe, M. Piquette, L. A., and M. Horányi, *Icarus* **221**, 135 (2012).

⁸ Y. Bailung et al., *Physics of Plasmas* **25**, 053705 (2018).

⁹ A. Dove et al., *Physics of Plasmas* **19**, 043502 (2012).

- ¹⁰ J. P. Sheehan et al., *Physical Review Letters* **111**, 75002 (2013).
- ¹¹ S. Langendorf and M. Walker, *Physics of Plasmas* **22**, 33515 (2015).
- ¹² S. F. Singer and E. H. Walker, *Icarus* **1**, 112 (1962).
- ¹³ J. J. Rennilson and D. R. Criswell, *The Moon* **10**, 121 (1974).
- ¹⁴ M. A. Pelizzari and D. R. Criswell, in *9th Lunar Planetary and Science Conference*, pages 3225–3237, 1978.
- ¹⁵ H. A. Zook and J. E. McCoy, *Geophysical Research Letters* **18**, 2117 (1991).
- ¹⁶ A. B. Binder, *Science* **281**, 1475 (1998).
- ¹⁷ O. E. Berg, H. Wolf, and J. Rhee, in *Interplanetary Dust and Zodiacal Light*, edited by H. Elssser and H. Fetching, page 233, Springer-Verlag, New York, 1976.
- ¹⁸ P. D. Feldman and D. Morrison, *Geophysical Research Letter* **18**, 2105 (1991).
- ¹⁹ O. E. Berg, F. F. Richardson, and H. Button, in *Apollo 17 Preliminary Science Report*, NASA Space. Publ. SP-330, 16-1-16-9, 1973.
- ²⁰ J. S. Halekas, Y. Saito, D. G. T., and F. W. M., *Planetary and Space Science* **59**, 1681 (2011).
- ²¹ G. C. Das, R. Deka, and M. P. Bora, *Physics of Plasmas* **23**, 042308 (2016).
- ²² S. K. Mishra and S. Misra, *Physics of Plasmas* **25**, 023702 (2018).
- ²³ X. Wang, J. Schwan, H.-W. Hsu, E. Grüm, and M. Horányi, *Geophysical Research Letters* **43**, 6103 (2016).
- ²⁴ S. Joseph, Undergraduate Honors Theses, 1442, University of Colorado at Boulder, 2017.
- ²⁵ M. Horányi, *Annual Review of Astronomy and Astrophysics* **34**, 383 (1996).
- ²⁶ H. A. Zook, A. E. Potter, and B. L. Cooper, in *Lunar and Planetary Science Conference*, volume 26, pages 1577–1578, 1995.
- ²⁷ R. Z. Sagdeev, in *Reviews of Plasma Physics*, edited by M. A. Leontovich, volume 4, page 23, Consultants Bureau, New York, 1966.
- ²⁸ P. K. Shukla and A. A. Mamun, Institute of Physics, Bristol and Philadelphia, 2002.
- ²⁹ B. M. Feuerbacher, B. F. Anderegg, L. D. Laude, R. F. Willis, and R. J. L. Grard, in *Lunar Science Conference*, volume IIIrd, pages 2655–2663, 1972.
- ³⁰ M. Horányi, B. Walch, S. Robertson, and D. Alwaxander, *Journal of Geophysical Research* **103**, 8575 (1998).
- ³¹ S. I. Popel et al., *JETP Letters* **99**, 115 (2014).
- ³² T. M. Burinskaya, *Planetary and Space Science* **115**, 64 (2015).
- ³³ C. M. Hatzell and D. J. Scheeres, *JGRE* **118**, 116 (2013).
- ³⁴ D. J. McComas et al., *Geophysical Research Letters* **30**, 1517 (2003).
- ³⁵ X. Wang, M. Horányi, and S. Robertson, *Planetary and Space Science* **59**, 1791 (2011).
- ³⁶ T. M. Flanagan and J. Groree, *Physics of Plasmas* **13**, 123504 (2006).

